Journal of X-Ray Science and Technology 10 (2002) 95–106
IOS Press

Image segmentation via fuzzy object extraction and edge detection and its medical application

Yao Lin, Jie Tian and Huiguang He
AI Lab, Institute of Automation, Chinese Academy of Sciences, Beijing POB 2728, 100080, China
Tel.: +86 10 82618465; Fax: +86 10 85191212; E-mail: tian@doctor.com

Abstract. A new interactive segmentation method that combines fuzzy connected object extraction and edge detection is proposed. Fuzzy connectedness is a global fuzzy relation, which effectively captures fuzzy "hanging togetherness" of image elements. First, by selecting the seed point, fuzzy connectedness value between each image element and the seed point is computed via dynamic programming. Then, through adjusting the parameter, the different fuzzy connected object could be extracted. Finally, an edge detection method is adopted to detect the object boundary. The algorithm is demonstrated on some medical images: segmentation of knee tissues in CT image and segmentation of brain tissues in MR image. The results show that this method works well for some CT and MR images.

1. Introduction

Segmentation, one of the bottlenecks of medical image processing, is a fundamental building block for higher-level image analysis, but it remains an open research problem. Because of the limitation of parametric resolution, the bias field of imaging devices and the movement of the subject, this creates inaccuracy and artifacts such as noise, blurring, and shading in the acquired images, especially in MR images.

Artifacts and inhomogeneities of medical images, have attracted the interest of researchers in fuzzy segmentation algorithms where a pixel may be classified partially into multiple classes [4,7]. The fuzzy C-means algorithm [5] (FCM) allows pixels to belong to multiple classes with varying degrees of membership via fuzzy pixel classification. However, it does not address the intensity inhomogenous artifact that occurs in nearly all MR images. In the fuzzy threshold methods, the image thresholds are usually selected by optimization of a well-designed fuzzy measurement, such as fuzzy c-partition entropy [3] and the measure of fuzziness [10]. Here, our study focused on the fuzzy connectedness-based method, which addressed the inhomogeneities of medical images.

Rosenfeld first proposed the concept of fuzzy connectedness in 1979. He extended the concept of connectedness to the theory of fuzzy sets. J.K. Udupa [8] extended the previously reported theory and presented a framework of fuzzy connected object definition. As we know, objects to be segmented in medical images are usually anatomical structures, which, often non-rigid and complex in shape, exhibit a considerable variability from person to person. Despite the blurred and inhomogenous medical image, observers are usually not difficult to recognize the anatomical structure, since image elements in the same object seem to hang together in nature. Intuitively, if the degree of hanging togetherness can be measured, the object of interest could be segmented easier. It means that the notion of hanging togetherness is very suitable for describing the anatomical structure in medical images. The concept of fuzzy connectedness can effectively capture the fuzzy "hanging togetherness" of image elements, which had been missing in the past segmentation research.

Humans other than computers have a better ability to recognize the object, but the latter can better delineate the object. To improve the accuracy of segmentation results, we presented a practical interactive segmentation method integrating region with edge information, in which the object to be segmented is specified by the user. We specialized the general definition of fuzzy connectedness to extract the object of interest. Like other traditional region-based method, it is often sensitive to the local noise in the image, resulting in small holes in the extracted region and sharp burrs on the boundary. To improve the segmentation result, we adopted an edge detection method in the next step. Applying this method to segment some CT images and MR images in the 3-D medical image processing system [13], the results showed that it performed well.

2. Basic fuzzy connectedness theory

For effectively addressing hanging togetherness, it is not enough to consider each image element on its own or in conjunction with its local neighbors. The spatial and topological relationship between each pair of image elements should be considered. A local fuzzy relation called affinity reflects the strength of local hanging togetherness between a pair of image elements. Fuzzy connectedness is a global fuzzy relation, which assigns the strength of global hanging togetherness to each pair (c, d) of image elements. Before presenting these fuzzy relations, we give some definitions in the theory of fuzzy subsets [8].

2.1. Fuzzy subsets, membership function, fuzzy relation

Let X be any reference set, a *fuzzy subset* M of X is a set of ordered pairs:

$$M = \{x, \mu_M(x))|x \in X\}, \quad \mu_M : X \to [0, 1], \tag{1}$$

where μ_M is the *membership function* of M in X.

A *fuzzy relation* ρ in X, ρ is a fuzzy subset of $X \times X$:

$$\rho = \{(x, y), \mu_\rho(x, y)|x, y \in X\}, \quad \mu_\rho : X \times X \to [0, 1] \tag{2}$$

For any fuzzy relation ρ in X, ρ is called a similitude relation in X if it is reflexive, symmetric and transitive.

2.2. Fuzzy spel adjacency, fuzzy digital space

Let n-dimensional Euclidean space-R^n be subdivided into hypercuboids by n mutually orthogonal families of parallel hyperplanes. The hypercuboid is called *spel* (an abbreviation for "space elements"). Without loss of generality, we assume that coordination of the center of each spel is an n-tuple of integer, which corresponds to a point in Z^n. If a fuzzy relation α in Z^n is reflexive and symmetric, it is said to be a *fuzzy spel adjacency*, which describes the spatial location relationship between the two spels. Commonly, $\mu_\alpha(c, d)$ is a non-increasing function of the distance $\|c - d\|$ between c and d.

We call the pair (Z^n, α) a *fuzzy digital space*. Fuzzy digital space is a concept that characterizes the underlying digital grid system independent of any image-related concepts.

2.3. Image scenes, membership scenes

An *image scene* S over a fuzzy digital space (Z^n, α) is a pair: $S = (C, f)$, where the spels in the image constitute a subset $C \subset Z^n$. f is a function whose domain is C and its range of values is a subset of integers. This function value of each spel reflects its image attribute (such as intensity).

We call C a *membership scene* over (Z^n, α) if the range of f is a subset of the unit interval $[0, 1]$.

2.4. Fuzzy spel affinity

Let $S = (C, f)$ be a membership scene over (Z^n, α). Any fuzzy relation κ in C is said to be a *fuzzy spel affinity* in S if it is reflexive and symmetric. In practice, the affinity between two spels is defined as the likelihood of their belonging to the same object in an image. Fuzzy spel affinity κ should to be such that $\mu_\kappa(c, d)$ is a function of $\mu_\alpha(c, d)$, the image attributes of c and d, and even the locations of c and d themselves. The general form of $\mu_\kappa(c, d)$ is:

$$\text{For all } c, d \in C,\ \mu_\kappa(c, d) = h(\mu_\alpha(c, d), f(c), f(d), c, d) \tag{3}$$

where h is a scalar-valued function with a range of $[0, 1]$. For computational reasons, however, we may have to bring in some restrictions.

2.5. Fuzzy κ-connectedness ξ

Let $S = (C, f)$ be a membership scene over (Z^n, α), and let κ be a fuzzy spel affinity in S. We define that the path $\rho(c, d)$ from c to d is a sequence of spels $< c^1, c^2, \ldots, c^m > (m \geqslant 2)$, for all c in C, such that $c^1 = c,\ c^m = d$. There are numerous possible paths between spel c and d. On each path p, there is a "weakest link" (in the sense of the smallest affinity μ_κ between successive pairs of spels along p) that determines the strength of connectivity along p. The actual "strength of connectivity" from c to d is the maximum of the "strength" of all paths. *Fuzzy κ-connectedness* in S is a fuzzy relation in C that assigns a value $\mu_\xi(c, d)$ to each pair (c, d). Let $P(c, d)$ denotes the set of all paths from the spel c to the spel d, $\mu_\xi(c, d)$ is defined as:

$$\mu_\xi(c, d) = \max_{\rho(c,d) \in P(c,d)} [\min(\mu_\kappa(c^1, c^2), \mu_\kappa(c^2, c^3), \ldots, \mu_\kappa(c^{m-1}, c^m))] \tag{4}$$

It is easy to prove that fuzzy connectedness ξ is a similitude fuzzy relation (reflexive, symmetric, and transitive) in C.

2.6. Fuzzy κ-component O_{θ_x}

To clarify the notion of a fuzzy connected component, we need to define binary relation ξ_θ based on the fuzzy connectedness ξ. We use θ to denote any subset of $[0, 1]$ and, for $0 \leqslant x \leqslant 1$; define $\theta_x = [x, 1]$.

Let $S = (C, f)$ be a membership scene over (Z^n, α), and let ξ be a fuzzy connectedness in S. For any c, $d \in C,\ x \in [0, 1]$ and any $\theta_x \subset [0, 1]$, we define a (hard) binary relation ξ_{φ_x} in C as follows:

$$\mu_{\xi_{\theta_x}}(c, d) = \begin{cases} 1, & \text{if } \mu_\xi(c, d) \in \theta_x \\ 0, & \text{otherwise} \end{cases} \tag{5}$$

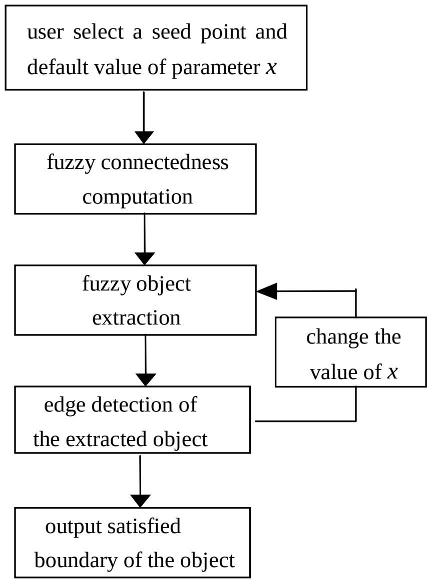

Fig. 1. Main steps of the algorithm.

It's easy to prove that ξ_{φ_x} is an equivalent relation in C. We denote $[o]_{\theta_x}$ as an equivalent class of the relation ξ_{φ_x} that contains o in C.

$$[o]_{\theta_x} = \{c \in C | \mu_\xi(o,c) \geqslant x\} \tag{6}$$

A fuzzy κ-component O_{θ_x} of S of strength θ_x containing o is a fuzzy subset of C defined by the membership function:

$$\mu_{O_{\theta_x}}(c) = \begin{cases} \eta(f(c)), & \text{if } c \in [o]_{\theta_x} \\ 0, & \text{otherwise} \end{cases}, \ \eta(f(c)) \in [0,1] \tag{7}$$

Given C, κ, ξ and $x \in [0,1]$, and any spel $o \in C$, we refer to the process of finding the fuzzy κ-component O_{θ_x} that contains o as fuzzy object extraction. In this paper, we also name O_{θ_x} as the fuzzy object.

3. Method description

Our method is an interactive method that combines fuzzy connected object extraction and edge detection (see Fig. 1). The parameter x is a number between 0 and 1, which represents the smallest fuzzy connectedness value between the seed point and the image spel in the fuzzy object of interest. If the value of x is smaller, the bigger fuzzy object O_{θ_x} is extracted. The method is briefly described as follows:

First, based on the seed point o selected by the user in the object region, the fuzzy connectedness value is computed between every spel to the starting point o. Second, a fuzzy connected component O_{θ_x} is extracted based on the value of x. At last, the boundary of the object is detected. If the result is not satisfied, the user can adjust the value of x to repeat the step 2 and 3.

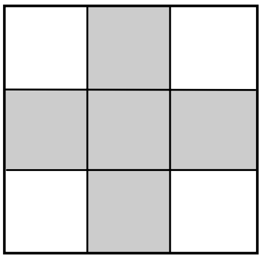

Fig. 2. 4-adjacency relation.

3.1. Fuzzy connectedness computation

To simplify computation, we adopt the following fuzzy spel adjacency and fuzzy spel affinity definition. In 2-D digital space, we adopt 4-adjacency relation as fuzzy spel adjacency (Fig. 2).

$$\mu_\alpha(c,d) = \begin{cases} 1, & \text{if } c = d \text{ or } c,d \text{ are 4-adjacent} \\ 0, & \text{otherwise} \end{cases} \tag{8}$$

In 3-D digital space, we adopt 6-adjacency relation as fuzzy spel adjacency.

$$\mu_\alpha(c,d) = \begin{cases} 1, & \text{if } c = d \text{ or } c,d \text{ are 6-adjacent} \\ 0, & \text{otherwise} \end{cases} \tag{9}$$

It is easily verified that these hard adjacency relations commonly used in digital topology are the special cases of the fuzzy spel adjacency.

The affinity framework provides us with a direct method of comparing the intensity and texture similarity in regions of an image. For the gray scale image, $\mu_\kappa(c,d)$ is defined as:

$$\mu_\kappa(c,d) = \mu_\alpha(c,d)\left[w_1 e^{-\frac{1}{2}\left(\frac{(f(c)+f(d)/2)-\mu_1}{\delta_1}\right)^2} + w_2 e^{-\frac{1}{2}\left(\frac{f(c)-f(d)-\mu_2}{\delta_2}\right)^2}\right] \tag{10}$$

where w_1, w_2 are the weighting parameters whose value are chosen by the user and satisfied $w_1 + w_2 = 1$, $f(c)$ is the intensity of spel c in the image scene. $\mu_1, \delta_1, \mu_2, \delta_2$ represent the mean and standard deviation of the intensity and their differences (gradient magnitude) in the scene for the spels in the object of interest. Of course, other than the intensity and gradient feature, different intensity-based features could be used in the definition of $\mu_\kappa(c,d)$, such as $\max(f(c), f(d)),\ \min(f(c), f(d)),\ |f(c) - f(d)|/(f(c) + f(d))$.

In the implementation, we computed the statistical parameters for the affinity function from a small neighborhood around the seed point specified by the user. We also allowed the user to select a few representative seeds in the object. All these seeds and the neighborhood around them were calculated statistically. When processing a large number of images of the same kind of anatomical structure (such as MR images of the brain), this estimation might be made once.

If rich texture exists in the image, we can add the texture feature to the definition. We take the co-occurrence matrix M to characterize the texture information. The texture similarity is measured by the norm of the difference of the two matrixes, i.e., $F(c,d) = \|M(c) - M(d)\|$. We can construct the multiple templates centered on randomly chosen spels in the neighborhood of the seed point. Subsequently, by computing the similarity between any pair of the templates, mean and standard deviation of texture similarity could be calculated.

In general, $\mu_\kappa(c, d)$ is defined as:

$$\mu_k(c, d) = \mu_\alpha(c, d) \sum_{i=1}^{T} w_i e^{-\frac{1}{2}\left(\frac{F_i(c,d)-\mu_i}{\delta_i}\right)^2} \tag{11}$$

where T is the number of the features in use, $F_i(c, d)$ indicates the i-th feature related to the spel c and d, μ_i and δ_i is respectively the mean and standard deviation of the i-th feature, and w_i is the parameter satisfying $\sum_{i=1}^{T} w_i = 1$.

The definition Eq. (10) shows that if the intensity difference between c and d is smaller and the average intensity of c and d is closer to the seed point, the value of $\mu_\kappa(c, d)$ is bigger. It means that c and d are more likely to belong to the same object. To understand intuitively, this definition is well designed.

The fuzzy connectedness of a pair of spels (c, d) is determined by traversing all the paths from c to d. Along each path, the minimum fuzzy affinity of the successive pair of elements is computed. The largest of these minimums is the fuzzy connectedness between c and d. Assume that the intensity in one object is slow varying, as what is often found in MR images due to magnetic field inhomogeneities, spels c and d are likely to have very different intensities although they are in the same object. Nevertheless, we can find a path from c to d such that intensities of each pair of successive spels on the path are very similar. This path indicates a strong connectedness between c and d. It demonstrates that fuzzy connectedness is robust to the inhomogeneities of medical images to some degree, because it considers the spatial relationship between each pair of image elements.

To reduce computing time, we applied the dynamic programming to compute fuzzy connectedness.

3.2. Fuzzy object extraction

After computing the fuzzy connectedness between each spel and the seed point, we can extract the fuzzy object. We can use the thresholding method (to select x) or cluster analysis to extract the fuzzy object of interest. In our method, we let the user to select the proper value of x.

As stated in Section 2, ξ_{φ_x} is an equivalence relation in C. This property ensures the repeatability and robustness of the algorithm. As long as the seed points selected by the user are in the same equivalence class of ξ_{φ_x}, the same fuzzy object O_{θ_x} can be extracted. So the location of the starting point in the same object has no effect on the segmentation result. It is important for practical use.

While the fuzzy object is extracted, we can get the corresponding image scene S. For any spel c in C, let:

$$f(c) = \begin{cases} G_{\max} \cdot \mu_\xi(o, c), & c \in [o]_{\theta_x} \\ 0, & c \notin [o]_{\theta_x} \end{cases}. \tag{12}$$

where $G_{\max}$ is the maximum feature value in the new image scene. Typically, its value is taken as 255 or 4095(according to the bit number of one pixel in the image scene).

Since we adopt the hard adjacency relation as fuzzy spel adjacency, it is only the direct adjacent spels that are taken into consideration in the procedure of computing fuzzy connectedness. In this way, it makes the value of fuzzy connectedness is sensitive to the local noise in the image. It might lead to noisy boundaries and holes in the interior of the object. To improve the segmentation result, we consider adopting an edge detection method to make the boundary smooth and remove the small holes in the object.

3.3. Edge detection

We have taken several edge detection methods, including some simple methods such as Sobel, Prewitt, Laplacian of Gaussian, Canny edge operator detecting, and some complex methods such as the live-wire [1] and snake method. We made a small modification to the Canny [9] method, and found it could produce good results in some cases. Thus, in this paper we only introduce the Canny method and its experimental results, while omitting the introduction of other methods.

The Canny operator was designed to be an optimal edge detector. It uses two thresholds to detect strong and weak edges, and includes the weak edges in the output only if they are connected to strong edges. Therefore it is likely to be better at detecting weak edges and less sensitive to noise.

Canny edge detection consists of three steps.

Step 1: Image smoothing

Since the gradient operator is of a high pass nature, and the noise is usually also in high frequencies it can sometimes create false edge pixels. Thus the image is first smoothed by the Gaussian function:

$$S[i,j] = G(i,j,\sigma) * I[i,j] \tag{13}$$

where I is the original image scene, G indicates the Gaussian function, σ is the stand deviation. However, Gaussian filtering will make edges blurring while eliminating the noise. To improve the accuracy of the edge detection, we use the anisotropic diffusion filtering [11] instead. It could not only eliminate the noise but also enhance the edge of image. The anisotropic diffusion equation is:

$$\frac{\partial I(x,y,t)}{\partial t} = \text{div}(g(\|\nabla I\|)\nabla I) = g(\|\nabla I\|)\Delta I + \nabla g \cdot \nabla I \tag{14}$$

where div is the divergence operator, $\|\nabla I\|$ is the gradient magnitude, and $g(\|\nabla I\|)$ is an "edge-stopping" function, which is used to adaptively control the smoothing. $g(\|\nabla I\|)$ is a nonnegative monotonically decreasing function, and chosen to satisfy $g(x) \to 0$ when $x \to \infty$ so that the diffusion is "stopped" across edges. It is often implemented in the form: $g(|\nabla I|) = 1/\sqrt{1 + |\nabla I|^2}$. In this manner, the image is smoothed without destroying the edges. Then the smoothed image is differentiated with respect to the x and y directions, and the gradient magnitude of each image spel is obtained.

Step 2: Non-maximum suppression

Since edges give rise to ridges in the gradient magnitude image, the edges are located at the points of local maximum. We need to suppress the non-maximum perpendicular to the edge direction, rather than parallel to the edge direction, since we expect the continuity of edge along an extended contour.

Step 3: Edge tracking

Although the image is smoothed, a few of false edges still exist in the non-maximum suppression image. The gradient magnitude of the false edge is lower than real edges. So the algorithm looks for pixels above a high threshold to locate real edges. However, in real images high gradient pixels are usually not neighbors. Then the algorithm traces the edges along all the paths so as to connect the strong edges by a path of pixels whose gradient magnitude are greater than a low threshold. In this way a thin line is given in the output. The tracking process exhibits hysteresis controlled by the two thresholds T1 and T2. This hysteresis helps to ensure that noisy edges are not broken up into multiple edge fragments.

In the implementation, J. Canny recommends the ratio of high to low threshold is in the range of two or three to one based on predicted signal-to-noise ratios. In the program pseudo-code shown in Section 3.4, the values of these parameters are selected based on our experiments.

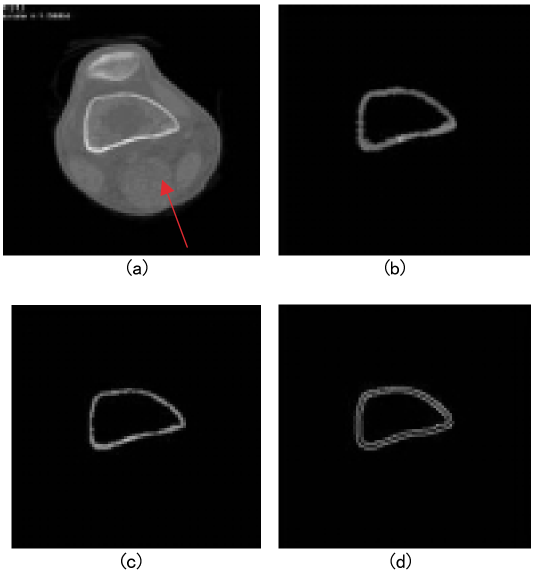

Fig. 3. Segmentation of the knee bone tissue. (a) a CT slice of a patient's knee, the seed point is selected in the left corner of knee bone region (indicated by the arrow); (b) connectivity scene of extracted fuzzy object O_{θ_x} based on a middle value of parameter x; (c) connectivity scene of extracted fuzzy object O_{θ_x} based on a higher value of x; d) satisfied boundary output of the bone region after canny edge detecting.

3.4. Efficient algorithm implementation

As previously mentioned, we utilize the dynamic programming method to compute fuzzy connectedness, which decreased the computational complexity through searching the optimum path from each image pixel to the seed point o. Then we use Canny edge detection method to obtain the object boundary. Due to the 2-D canny edge detector, this method is mainly used in 2D image segmentation. However, since the 3D fuzzy object is easily extracted, we can detect the boundary of the fuzzy object slice by slice. The main program pseudo-code of this method is as follow:

Input: Seed point o selected by the user
Output: Edge of object of interest containing the seed point o.
Auxiliary Data Structure: A queue Q of points.
Begin:

0. For any image pixel c
1.   set $fc[c] = 0$;
2. End for
3. $fc[o] = 1$;
4. Set the default value of parameter x;
5. Set $Q =$ empty queue, and push o to Q;
6. While Q is not empty
7.   Pop c from Q;
8.   for each immediate neighbor d of c
   $f_{\max} = \max_d \left(\min(fc(d), \mu_\kappa(c, d)\right)$
9. If $(f_{\max} > fc(c)$ and $f_{\max} \geqslant x)$

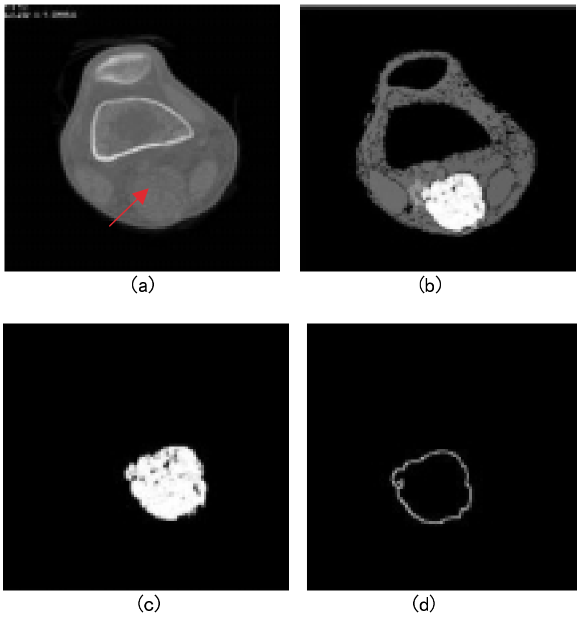

Fig. 4. Segmentation of the knee fat tissue. (a) a CT slice of a patient's knee, the seed point is selected in the middle of knee fat region (indicated by the arrow); (b) connectivity scene of extracted fuzzy object O_{θ_x} based on a middle value of x; (c) connectivity scene of extracted fuzzy object O_{θ_x} based on a higher value of x; (d) satisfied boundary output of the fat region after canny edge detecting.

10. Set $fc(c) = f_{\max}$;
11. If $\mu_k(c, d) > 0$
12. Push pixel d to Q;
13. End if
14. End if
15. End while
16. Get the membership scene (C, f_c) of fuzzy object containing o;
17. Canny (f_c, width, height, 0.35, 0.8);
18. If result is not satisfied
19. Change the value of parameter x;
20. Return step 16;
21. Else
22. Output satisfied boundary of object.
23. End if

End

4. Experiments and evaluation

4.1. Experiment results

This method was used in the medical image processing system (3DMED) developed by our lab. It has successfully segmented scores of CT images and MR images. Experimental results showed that edge

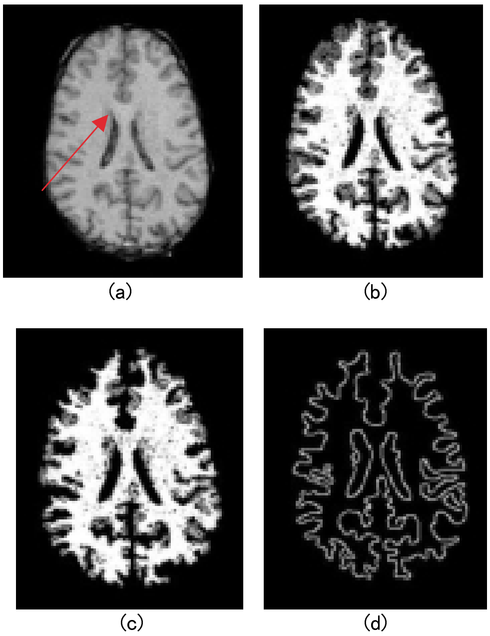

Fig. 5. Segmentation of the brain white matter. (a) a MR slice of a patient's brain; the seed point is selected in the middle of brain white matter region (indicated by the arrow); (b) connectivity scene of extracted fuzzy object O_{θ_x} based on a middle value of x; (c) connectivity scene of extracted fuzzy object O_{θ_x} based on a higher value of x; (d) satisfied boundary output of the white matter region after canny edge detecting.

detection method produces better segmentation results compared to those of threshold method. Some representative images are shown in Figs 3, 4 and 5.

4.2. Quantitative evaluation

To evaluate the segmentation results quantitatively and objectively, evaluation needs to be done based on the ground truth data [6]. We adopted the IBSR database freely downloaded from the Internet. The data of the Internet Brain Segmentation Repository are provided by the Center for Morphometrics Analysis at Massachusetts General Hospital. Both real MR brain scan data and corresponding ground truth segmentations are available at the IBSR website at: http://neuro-www.mgh.harvard.edu/cma/ibsr.

Since the output of the edge detection is a binary image consisting of boundary pixels, we evaluated the method by comparing a binary image containing true boundaries with another binary image containing segmented boundaries. According to Thomas C.M. Leey's evaluation method [12], we selected the Baddeley's Δ_w^p [2] as the distance measure for comparing such binary "boundary pixel images". Let X be a grid with N pixels, and let $A \subset X$ and $B \subset X$ be the set of all "black pixels" of a true and a fitted binary image respectively.

$$\Delta_w^p(A,B) = \left[\frac{1}{N}\sum |w(d(x,A)) - w(d(x,B))|^p\right]^{\frac{1}{p}} \tag{15}$$

where $d(x,A)$ is the smallest distance from x to A, $w(t) = \min(t,c)$ is a threshold function, and p and c are parameters supplied by the user. We followed Baddeley and set $p = 2$ and $c = 5$.

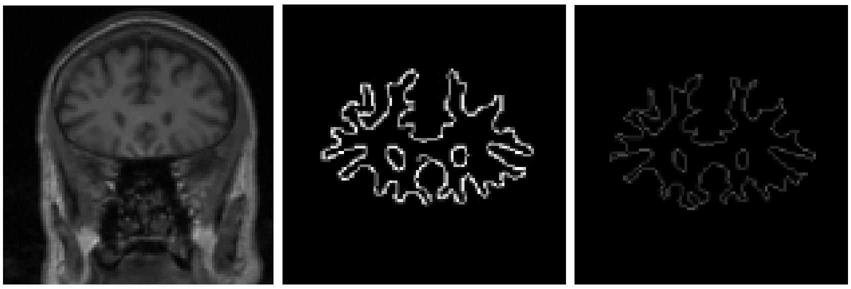

(a) segmentation of slice 44

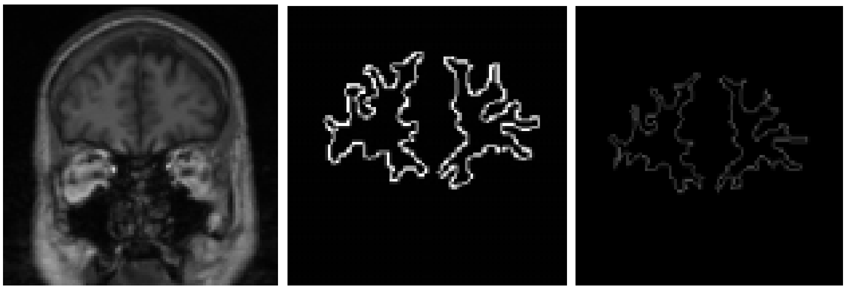

(b) segmentation of slice 49

Fig. 6. Segmentation of the brain white matter in MR images from IBSR.

Table 1
The Baddeley's distance measures

	Slice 43	Slice 44	Slice 45	Slice 46	Slice 47	Slice 48	Slice 49
Distance measure	0.357766	0.267986	0.269025	0.276055	0.258095	0.289075	0.268015

The dataset 788_6_m is a T1-weighted three dimensional coronal brain scan after it has been positionally normalized. The MRI scan was acquired for a 55 year old male subject with a 1.5 Tesla General Electric Signa. It contains 60 contiguous 3.0 mm slices. We give the segmentation result of the "white matter" tissue in some slices from this dataset (Fig. 6). The left column is the original image; the middle one is the segmentation of our method; the right one is the ground truth segmentation. We compute the Baddeley's distance between the segmentation result of our method and the ground truth segmentation, and enumerate the evaluation results in Table 1.

5. Conclusion

In this paper, we proposed a practical two-stage method integrating fuzzy connected object extraction with edge detection, and applied it to segment medical images. Some image intensity-based features, such as texture feature were introduced into the fuzzy affinity definition. Moreover, Canny edge detection method was modified by adopting anisotropic diffusion filtering. Experiment results show that the method is feasible to medical images and deserves further research. It could be used to segment the white matter, tumor tissue and other small and simple structured organs in CT and MR images. Next, we would integrate fuzzy connectedness based method with the EM algorithm and geometrical deformable model to make it applicable to more kinds of medical images and have better robustness to noise.

Acknowledgments

We are grateful to the editors, anonymous reviewers and Prof. Qian Shouchu for their careful reading and helpful suggestions. Thanks for the Center for Morphometrics Analysis at Massachusetts General Hospital who provided the IBSR database. This research was supported by the National Natural Science Foundation of China under Grant No. (69931010; 60071002; 60072007; 60172057).

References

[1] A.X. Falcao, J.K. Udapa, S. Samarasekera and B.E. Hirsch, User-steered image boundary segmentation, *Proceedings of SPIE on Medical Imaging*, Newport Beach, CA, 2710, 1996, pp. 278–288.
[2] A.J. Baddeley, Errors in binary images and an L^p version of the Hausdorff metric, *Nieuw Archief voor Wiskunde*, 1992, pp. 157–183.
[3] J.-R. Chen and J. Li, Threshold selection based on fuzzy c-partition entropy approach, *Pattern Recognition* **31**(7) (1998), 857–870.
[4] D.L. Pham, C. Xu and J.L. Prince, A survey of current methods in medical image segmentation, Technical Report JHU/ECE 99-01, University of Johns Hopkins, 1998.
[5] D. Pham and J. Prince, An adaptive fuzzy segmentation algorithm for three-dimensional MRI, *Information Processing in Medical Imaging* (1999), 140–153.
[6] E.B. Dam, Evaluation of diffusion schemes for multiscale watershed segmentation, MSC. Dissertation, University of Copenhagen, 2000.
[7] J.S. Duncan and N. Ayache, Medical image analysis: progress over two decades and the challenges ahead, *IEEE Transaction on Pattern Analysis and Machine Intelligence* **22**(1) (2000), 85–104.
[8] J.K. Udupa and S. Samarasekera, Fuzzy connectedness and object definition: theory, algorithms and applications in image segmentation, *Graphical Model and Image Processing* **58**(3) (1996), 246–261.
[9] J. Canny, A computational approach to edge detection, *IEEE Transactions on Pattern Analysis and Machine Intelligence* **8**(6) (1986), 679–698.
[10] L.-K. Huang and M.-J.J. Wang, Image thresholding by minimizing the measure of fuzziness, *Pattern Recognition* **28**(1) (1995), 41–51.
[11] P. Perona and J. Malik, Scale space and edge detection using anisotropic diffusion, *IEEE Transactions on Pattern Analysis and Machine Intelligence* **12** (1997), 629–639.
[12] T.C.M. Leey, A minimum description length based image segmentation procedure and its comparison with a cross-validation based segmentation procedure, Department of Statistics, University of Chicago, 1997.
[13] Three-dimensional medical image processing system (3DMED), Technique Report, Institute of automation, Chinese academy of sciences, http://www.3dmed.net.